STUDIA UBB CHEMIA, LXXI, 2, 2026 (p. 125-145)
(RECOMMENDED CITATION)
DOI:10.24193/subbchem.2026.2.07

PHOTOCHEMICAL SELF-PURIFICATION OF AQUATIC SYSTEMS IN THE PRESENCE OF VITAMIN B_6

Viorica GLADCHI[a], Vladislav BLONSCHI[a], Gheorghe DUCA[b], Angela LIS[a,*], Radu SILAGHI-DUMITRESCU[c]

ABSTRACT. Vitamin B_6 (pyridoxine, PN) released from anthropogenic and biogenic activities can influence the chemical self-purification of surface waters through its photochemical transformations. The present study aimed to investigate the kinetics and mechanisms of pyridoxine photodegradation under conditions that partially simulate the natural environment (pH ~7, aerated medium) using simulated solar irradiation. Three model systems were investigated: (1) *PN–hv*; (2) *PN–H_2O_2–hv*; (3) *PN–H_2O_2–Cu(II)–hv*, using direct spectrophotometry (λ = 328 nm). The kinetic parameters determined included partial reaction orders (using the van't Hoff method), effective rate constants, and half-lives ($\tau_{1/2}$). Direct photolysis of PN follows a partial reaction order of 0.2 with respect to [PN], with $k = (5.38\pm0.26)\cdot10^{-4}$ s^{-1} and $\tau_{1/2}$ = 21±0.5 min. However, the low quantum yields $(7.31–10.70)\cdot10^{-3}$ indicate that direct photolysis of vitamin B_6 is negligible under natural aquatic conditions. In the presence of H_2O_2, the partial reaction orders are 0.3 (PN) and 0.7 (H_2O_2), with $W = k\cdot[PN]^{0.3}\cdot[H_2O_2]^{0.7}$, $k = (3.69\pm0.11)\cdot10^{-4}$ s^{-1} and $\tau_{1/2}$ = 31.1±0.30 min. For *PN–H_2O_2–Cu(II)*, the partial reaction orders are 0.2 (PN), 0.4 (H_2O_2), and 0.3 (Cu^{2+}) with $k = (3.91\pm0.17)\cdot10^{-4}$ s^{-1}, and $\tau_{1/2}$ = 29.2±0.53 min. In conclusion, PN undergoes measurable photodegradation under simulated natural conditions.

Keywords: *Vitamin B_6, pyridoxine, photolysis, H_2O_2, Cu(II), water self-purification, reaction kinetics.*

[a] *Moldova State University, Faculty of Chemistry and Chemical Technology, 60 Mateevici str., MD-2009, Chisinau, Republic of Moldova*
[b] *Moldova State University, Institute of Chemistry, 3 Academiei str., MD-2028, Chisinau, Republic of Moldova*
[c] *Department of Chemistry and Chemical Engineering, Babes-Bolyai University, 11 A. Janos Street, RO-400028, Cluj-Napoca, Romania*
* *Corresponding author: angela.lis@usm.md*

INTRODUCTION

The increasing anthropogenic impact on aquatic ecosystems leads to the deterioration of their physicochemical characteristics. The problem is compounded by the fact that the self-purification capacity of these water systems is significantly lower (and continues to make it smaller) with respect to the quantity and quality of pollutants entering them.

Water self-purification can occur through multiple physical, biological and chemical processes. Among these, chemical self-purification in the upper layers of water under sunlight is particularly important, as it can be achieved through photochemical degradation of pollutants.

Water pollution with organic matter is a pressing problem that requires continuous evaluation and investigation. Therefore, it is important to study the role of various pollutants with reducing properties in the photochemical processes of water self-purification. Vitamins, including vitamin B_6, are among these substances. Vitamin B_6 in natural waters is present as a result of metabolic processes of aquatic organisms, discharges from the pharmaceutical industry producing food additives, and municipal wastewater. Vitamin B_6 concentrations in natural waters are generally very low and depend on several natural and anthropogenic factors [1, 2]. In the neutral or weakly alkaline environment characteristic of natural waters, pyridoxine (PN) is the most stable form of vitamin B_6 [3-8].

In the surface layers of water, photolysis is a predominant pathway of chemical self-purification. Photolytic transformations in nature occur under the influence of ultraviolet radiation. For most organic pollutants, maximum spectral activity occurs within the wavelength range of 310–350 nm [9-10]. Photochemical transformations of pollutants may proceed via direct, induced, or sensitized photolysis.

Direct photolysis occurs when a pollutant (P) undergoes chemical transformation under the influence of sunlight, according to the equation [9-10]:

$$\mathrm{P} + h\nu \rightarrow \mathrm{P}^{*} + Products \quad (1)$$

Induced photolysis is characterized by the oxidation of P by free radicals formed during the decomposition of photoinitiator molecules under the influence of sunlight. In aqueous media, the most common photoinitiator is hydrogen peroxide (H_2O_2), so the reaction process can be represented as follows [9-10]:

$$\mathrm{H_2O_2} + h\nu \rightarrow 2\bullet\mathrm{OH} \quad (2)$$

$$2\bullet\mathrm{OH} + \mathrm{P} \rightarrow Products \quad (3)$$

Another pathway of photochemical transformation of pollutants in aquatic environments is sensitized photolysis, which involves the participation of sensitizing species (S):

$$S + hv \rightarrow S^* \quad (4)$$

$$S^* + \mathrm{P} \rightarrow Products \quad (5)$$

The behavior of vitamin B_6 in aquatic systems has been poorly studied. Therefore, understanding its role in the photochemical self-purification processes of natural waters is of considerable importance.

RESULTS AND DISCUSSION

Direct photolysis

For the direct photolysis of vitamin B_6 (pyridoxine, PN) under the established conditions, the kinetic parameters of the process were determined, including the partial reaction order with respect to the substrate concentration (Figure 1).

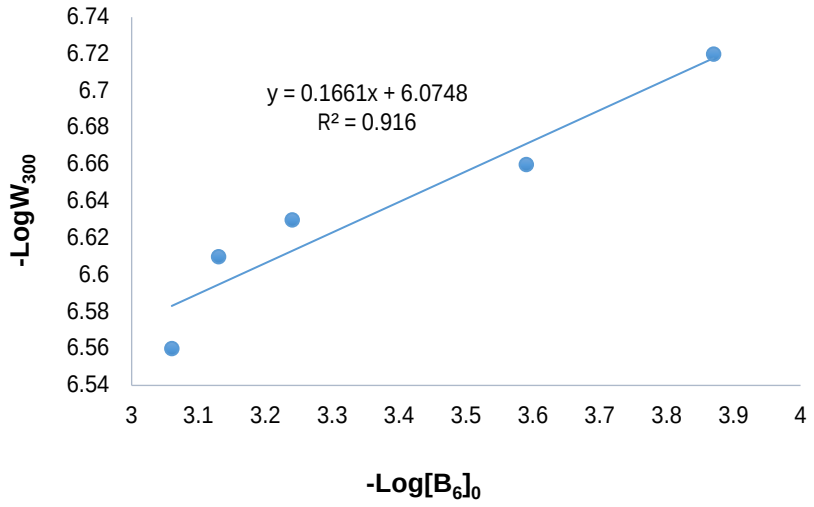

Figure 1. Determination of the partial reaction order (log-log plot of rate vs. [B_6]) for the photochemical oxidation of vitamin B_6 (20^0C, pH = *const.* = 7). Radiation source: Oriel Solar Simulator, AM1.5D filter [own data]

The data used to determine the reaction order with respect to the concentration of vitamin B_6 during direct photolysis are presented in Table S.1. The partial reaction order for the direct photolysis of vitamin B_6 was found to be 0.2. Therefore, the mathematical expression describing the reaction rate can be written as follows:

$$W = \kappa \cdot [B_6]^{0.2} \quad (6)$$

The effective rate constant (at different concentrations of components in the systems) depends on several factors, including temperature, dissolved oxygen concentration, and pH.

Under the experimental conditions employed in this study, the effective rate constant for the direct photolysis of vitamin B_6 was calculated to be $k = (5.38 \pm 0.26) \cdot 10^{-4}$ s^{-1}. Based on this value, the half-life of the process was determined to be $\tau_{1/2} = 21.0 \pm 0.5$ min.

Previous studies have investigated the photochemical transformations of vitamin B_6 under similar conditions and identified the products formed during direct photolysis [11-13] (Table 1).

Table 1. Vitamin B_6 (pyridoxine) photoproducts under various conditions

Conditions	Radiation sources	The main products of photolysis	Comments/ mechanisms	Bibliographic source
pH 7.0, O_2 present	UV (254–300 nm)	4-Pyridoxic acid (4-PA), traces of pyridoxal	The quantum yield is low; quinone-methide formation as intermediates	[11]
pH 7.0, O_2 present	UV (313–365 nm)	4-PA, lactone derivatives, dehydropyridoxine	The main pathway is hydrolysis of the quinone-methide intermediates	[12]
pH 5–9	UV (290–350 nm)	Traces of pyridoxal-5-phosphate (due to hydrolysis), 4-PA	The quantum yield is very low; the protonation configuration is important	[13, 14]
pH 7.0, O_2 present	UVC (254 nm)	Chain termination with the formation of low molecular weight organic acids	Direct photolysis with radical products (C–N and C–C cleavages)	[11]

Therefore, the existing literature indicates several possible products of vitamin photodegradation that may be confirmed or ruled out in future research.

The determination of the light intensity emitted by the solar simulator is essential for the quantitative evaluation of photochemical transformations of vitamin B_6 in aqueous solution. The efficiency of light energy utilization in photochemical reactions is characterized by the quantum yield, which is defined as the ratio between the amount of product formed and the amount of absorbed light during irradiation. Therefore, accurate determination of the photon flux emitted by the irradiation source is necessary for the calculation of the quantum yield of direct photolysis.

For this purpose, the photon flux of the Solar Simulator was determined using the potassium ferrioxalate(III) chemical actinometer, $K_3[Fe(C_2O_4)_3]\cdot 3H_2O$ (Table 2). The use of this actinometer was appropriate because potassium ferrioxalate(III) is sensitive in the spectral range of 250–480 nm, while vitamin B_6 exhibits a maximum absorption at 328 nm, which falls within this interval. The synthesized chemical actinometer was irradiated under the same experimental conditions as the studied system, and the photon flux was subsequently calculated. Simultaneously, a control sample of identical composition that was not exposed to irradiation was monitored. No formation of Fe(II) ions was observed in the control sample, confirming that the photochemical transformation occurred only under irradiation.

Table 2. Luminous flux and energy flux of Solar Simulator Oriel 9119X, AM1.5D filter

$[K_3[Fe(C_2O_4)_3]]$	ϕ	$\Delta n\ (Fe^{2+})/\Delta t \cdot 10^8$, mol·s^{-1}	$I_{avg.}$ (photon flux)·10^8, Einstein·s^{-1}	$I_{avg.}$ (photon flux)·10^6, Einstein·L^{-1}·s^{-1}	Luminous flux·10^8, Einstein·cm^{-2}·min^{-1}	Energy flux·10^2, Joules·cm^{-2}·min^{-1}
0.006 M	1.26	32.90	26.10	26.10	124.00	58.00
0.012 M	1.26	32.80	26.00	26.00	124.00	58.00
0.015 M	1.26	32.80	26.00	26.00	124.00	58.00

The obtained results indicate that the photon flux emitted by the Solar Simulator equipped with the AM 1.5D filter was $(26.10\pm0.06)\cdot 10^{-6}$ Einstein·L^{-1}·s^{-1}. Based on the irradiated surface area, it was also possible to calculate the average light intensity, luminous flux, and energy flux of the irradiation source (Table 2). The obtained data confirmed that the emitted radiation intensity does not depend on the initial concentration of the chemical actinometer or on traces of impurities, since very close results were obtained for three different concentrations of potassium ferrioxalate(III).

To evaluate the probability and efficiency of direct photolysis of vitamin B_6 in aqueous systems, the quantum yields of the process were determined for all investigated concentrations (Table 3).

Table 3. Kinetic parameters of the vitamin B_6 direct photolysis

$[B_6]_0 \cdot 10^4$, M	$W_{300} \cdot 10^7$, $M \cdot s^{-1}$	$\phi \cdot 10^3$	$k \cdot 10^4$, s^{-1}	$\tau_{1/2}$, min
1.34	1.90	7.31	5.38±0.26	21.0±0.5
2.56	2.20	8.46		
5.73	2.33	8.96		
7.34	2.47	9.50		
8.64	2.78	10.70		

The obtained results showed that the quantum yield of vitamin B_6 direct photolysis is significantly lower than unity and decreases with decreasing substrate concentration in solution. This behavior may be explained by the fact that the process occurs in dilute aqueous solutions (10^{-4} M), where photoexcited molecules are efficiently deactivated through collisions with solvent molecules, resulting in non-radiative energy dissipation.

The determined quantum yield values, ranging from $7.31 \cdot 10^{-3}$ to $10.70 \cdot 10^{-3}$, indicate a relatively low probability of direct photochemical transformation of vitamin B_6 under the studied conditions. Although the calculated half-life values demonstrate that the substrate undergoes measurable degradation under irradiation, the low quantum yield suggests that only a small fraction of absorbed photons effectively initiates photochemical conversion. Extrapolating the results obtained under laboratory conditions to real environmental conditions, it can be concluded that the direct photolysis of vitamin B_6 in natural waters is relatively limited, especially considering that the concentration of vitamin B_6 in aquatic environments is usually very low, typically ranging from pM to nM levels. Moreover, the efficiency of this process is influenced by environmental factors such as cloudiness, time of day, season, solar radiation intensity etc. Therefore, under natural aquatic conditions, the contribution of direct photolysis to the degradation of vitamin B_6 may be considered negligible.

Photolysis of vitamin B_6 in the presence of hydrogen peroxide

It is known that the chemical composition of natural waters also includes hydrogen peroxide, which ensures their dynamic redox balance and the content of which varies in the range of 10^{-5}-10^{-7} M. When exposed to UV radiation in the range of 300-310 nm, photolytic decomposition of hydrogen peroxide occurs with the formation of $OH^{\cdot}$ radicals:

$$H_2O_2 + h\nu \rightarrow 2HO^{\bullet} \quad (7)$$

$$H_2O_2 + HO^{\bullet} \rightarrow HO_2^{\bullet} + H_2O \quad (8)$$

Therefore, it is of interest to investigate the influence of hydrogen peroxide on the photodegradation of vitamin B_6 under conditions inspired by the composition of natural waters. This was achieved by modeling the system consisting of a solution of vitamin B_6 and hydrogen peroxide at pH 7.0, which was subjected to irradiation with a Solar Simulator with a filter which simulates the amount of solar energy and the wavelength of UV rays reaching the soil surface. The concentration of vitamin B_6 was varied in the range of 10^{-4} M, and of hydrogen peroxide in the range of 10^{-5} M.

To determine the partial reaction order of the induced photolysis with respect to the concentration of vitamin B_6, the required data were calculated, as presented in Table S.2. The partial reaction order was determined graphically from the dependence of ($-\log W_{300}$) on ($-\log C_{B6}$). The slope of the resulting linear plot with respect to the x-axis corresponds to the partial reaction order and was found to be 0.3 (Figure 2).

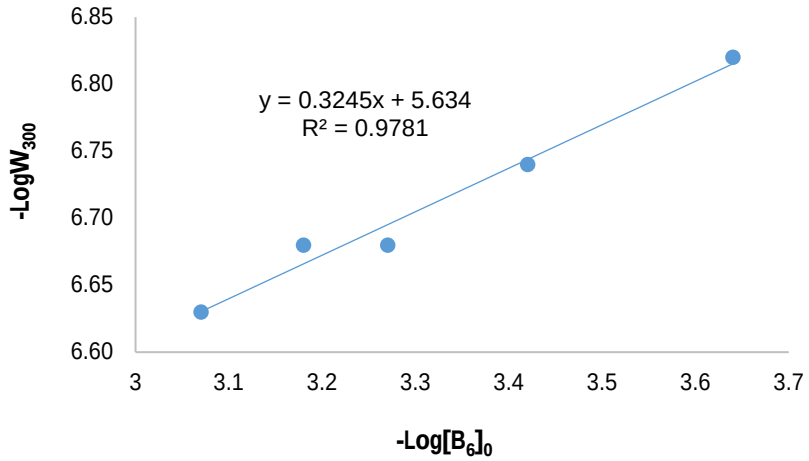

Figure 2. Determination of the partial reaction order (log-log plot of rate vs. [B_6]) for the photodegradation of vitamin B_6 in the presence of hydrogen peroxide ([H_2O_2] = *const.* = $3 \cdot 10^{-5}$ M, 20^0C, pH = *const.* = 7). Radiation source: Oriel Solar Simulator, AM1.5D filter [own data]

Similarly, the data required to determine the partial reaction order of induced photolysis with respect to the concentration of hydrogen peroxide were obtained and are presented in Table S.3. The partial reaction order with respect to hydrogen peroxide was determined to be 0.7 (Figure 3).

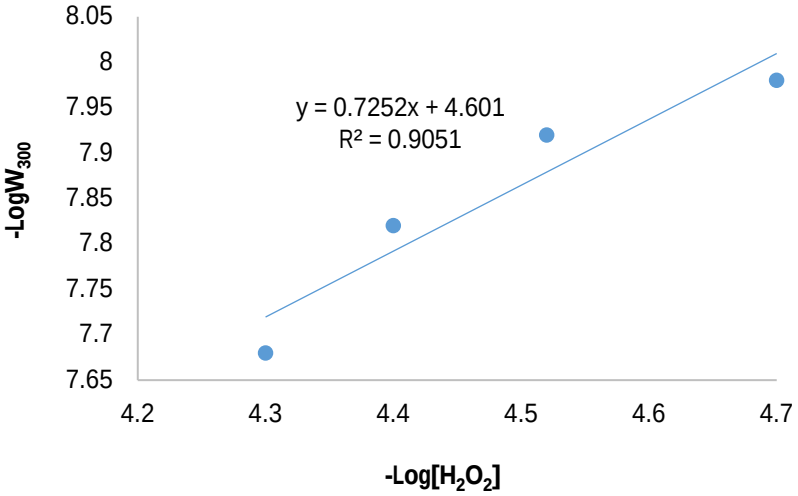

Figure 3. Determination of the partial reaction order (log-log plot of rate vs. $[H_2O_2]$) for the photodegradation of vitamin B_6 in the presence of hydrogen peroxide ($[B_6]$ = *const*. = $3 \cdot 10^{-4}$ M, 20^0C, pH = *const*. = 7). Radiation source: Oriel Solar Simulator, AM1.5D filter [own data]

Consequently, the following kinetic equation describing the dependence of the reaction rate on the concentrations of the system components was derived:

$$W = \kappa \cdot [B_6]^{0.3} \cdot [H_2O_2]^{0.7} \quad (9)$$

where: k – the rate constant (s^{-1}), which is influenced by temperature, dissolved oxygen concentration in water, and pH value.

For the photooxidation of vitamin B_6 in the presence of hydrogen peroxide, the effective rate constant was calculated to be $(3.69 \pm 0.11) \cdot 10^{-4}$ s^{-1} at various concentrations of the system components. Based on this value, the half-life was determined to be 31.1±0.3 min.

Upon irradiation of a mixture of pyridoxine and hydrogen peroxide, the initial stage involves the photolysis of hydrogen peroxide with the formation of hydroxyl radicals [15]. These radicals subsequently interact with the substrate and promote its degradation. Data reported by several authors who investigated the photolysis of vitamin B_6 in the presence of hydrogen peroxide [13, 16–20] indicate the formation of several products, including pyridoxal, 4-pyridoxic acid, and other low-molecular-weight compounds (Table 4).

Table 4. Possible products of photolysis of pyridoxine (vitamin B_6) in the presence of H_2O_2

Product	Formation mechanism	Bibliographic source
Pyridoxal (PL)	•OH attack on the $–CH_2OH$ group → formation of an aldehyde	[20-28]
4-Pyridoxic acid (4-PA)	Oxidation of the aldehyde group → carboxylic acid	[13, 17]
6-Hydroxy-pyridoxine (6-OH-PN)	Hydroxylation of the aromatic ring •OH	[18]
Pyridoxyquinone-type products	Oxidation of the aromatic ring → quinone-like products	[19]
Peroxide adducts (hydroperoxide, endoperoxide)	Adduct formation with $^1O_2$ or •OH; unstable intermediates	[19]
Small acids (formic, oxalic), CO_2	Mineralization in excess of •OH	[20]
Fragmentation (isopyridoxal etc.)	C–N and C–C bond cleavage	[28]

Analysis of the effective rate constants and half-lives for the direct photolysis of pyridoxine and its photolysis in the presence of hydrogen peroxide shows that the second process proceeds less efficiently (Table 5).

Table 5. Effective constant and half-life of pyridoxine (vitamin B_6) photolysis under various conditions [own data]

System	Effective constant (k), s^{-1}	Half-life ($\tau_{½}$), min
Pyridoxine-hv	$(5.38±0.25)\cdot10^{-4}$	21.0±0.5
Pyridoxine-H_2O_2-hv	$(3.69±0.11)\cdot10^{-4}$	31.1±0.3

The obtained results can be theoretically explained on the basis of previous studies conducted in this field [4, 13, 14, 19-21]. In aqueous solution, pyridoxine (PN, vitamin B_6) undergoes direct photolysis mainly through photoexcitation of the pyridine chromophore, leading to oxidation to pyridoxal (PL) and subsequently to products such as pyridoxic acid (4-PA). However, when hydrogen peroxide (H_2O_2) is present, the observed rate of PN photodegradation decreases.

Several photophysical and photochemical factors may account for this inhibitory effect. One possible explanation is the UV-screening effect of H_2O_2. Hydrogen peroxide absorbs UV radiation below 300 nm, partially overlapping with the absorption spectrum of PN. As a result, the intensity of

UV radiation available to excite PN molecules is reduced, thereby decreasing the rate of direct photolysis. However, since PN is present in the reaction mixtures at concentrations approximately one order of magnitude higher than those of hydrogen peroxide and exhibits significantly higher molar extinction coefficients owing to its aromatic structure, the shielding effect is expected to contribute only marginally to the observed inhibition.

The reduced efficiency of vitamin photooxidation may also be associated with limited radical generation and radical recombination processes. Although H_2O_2 can generate hydroxyl radicals (•OH) upon photolysis, this process proceeds relatively slowly in neutral aqueous media in the absence of a catalyst. Furthermore, radical recombination (•OH + •OH → H_2O_2) decreases the concentration of reactive species available for PN oxidation [22–24].

Finally, in the absence of metal catalysts, the distribution of reactive oxygen species (ROS) may differ, further reducing the efficiency of substrate photooxidation. Without Cu^{2+} or Fe^{3+} ions, H_2O_2 remains relatively stable under irradiation. Thus, although it acts as an oxidant in catalytic (Fenton-like) systems, in a simple *PN–H_2O_2* photolysis system hydrogen peroxide may instead suppress the direct photochemical degradation of PN [19].

Taken together, these considerations explain why the direct photolysis of pyridoxine proceeds more efficiently than photolysis in the presence of hydrogen peroxide. Nevertheless, these hypotheses require further verification and should be confirmed by additional experimental evidence obtained using modern analytical techniques.

Photolysis of vitamin B_6 in the presence of H_2O_2 and Cu^{2+} ions

An important component of the chemical composition of natural waters is Cu^{2+} ions, which act as effective catalysts in pollutant transformation reactions occurring during chemical self-purification processes. The Cu^{2+}/Cu^{+} redox couple exhibits a catalytic effect in numerous oxidation–reduction systems. It is also known that Cu(II) complexes, upon irradiation, can form excited species capable of promoting substrate oxidation, according to the following reaction [25]:

$$Cu(II)\text{-}L + h\nu \rightarrow Cu(II)\text{-}L^{\cdot} \rightarrow Cu(I) + L^{+} + e \qquad (10)$$

At the same time, Cu(I) ions promote the generation of additional hydroxyl radicals (•OH), according to the following equation [25]:

$$Cu(I) + H_2O_2 \rightarrow Cu(II) + HO^{\bullet} + OH^{-} \qquad (11)$$

Therefore, to more realistically simulate natural water conditions, a model system was designed in which the kinetic behavior of pyridoxine photodegradation was investigated in the presence of hydrogen peroxide and Cu^{2+} ions. Under neutral conditions (pH ≈ 7.0), the concentration of pyridoxine was 10^{-4} M, while the concentrations of hydrogen peroxide and Cu^{2+} ions varied within the range of $1.0 \cdot 10^{-6}$ - $5.0 \cdot 10^{-6}$ M.

Similarly to the previous systems, the initial rates of the modeled photochemical processes were determined (Tables S.4–S.6). The differential Van't Hoff method was used to calculate the partial reaction orders. Based on the experimental data, plots of lgW_{300} the logarithm of concentration were constructed for each varying system component. The partial reaction order was determined from the slope of the resulting linear plot with respect to the x-axis (Figures 4–6).

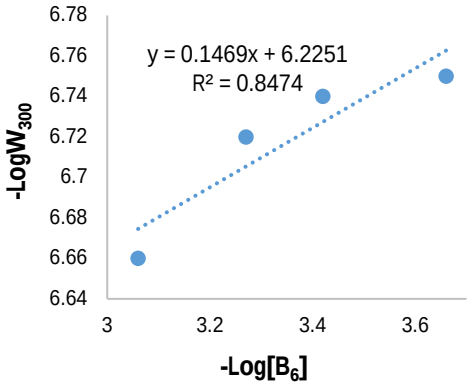

Figure 4. Dependence of the negative logarithm of the reaction rate of vitamin B_6 photooxidation on the negative logarithm of its concentration in the system under the influence of UV radiation. $[H_2O_2]$ = *const.* = $3 \cdot 10^{-5}$ M; $[Cu^{2+}]$ = *const*. = $3 \cdot 10^{-6}$ M. Radiation source: Oriel Solar Simulator, AM1.5D filter [own data]

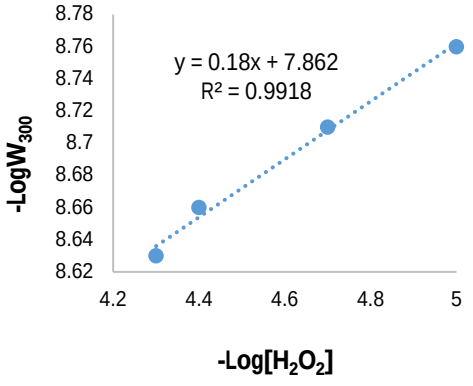

Figure 5. Dependence of the negative logarithm of the photooxidation reaction rate of vitamin B_6 on the negative logarithm of the hydrogen peroxide concentration in the system under the influence of UV radiation. $[B_6]$ = *const*. = $3 \cdot 10^{-4}$ M; $[Cu^{2+}]$ = *const*. = $3 \cdot 10^{-6}$ M. Radiation source: Oriel Solar Simulator, AM1.5D filter [own data]

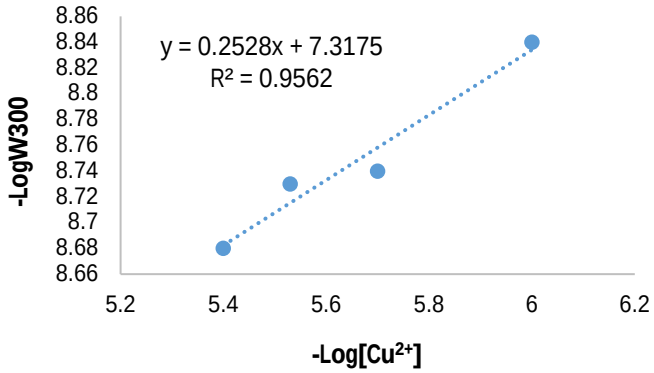

Figure 6. Dependence of the negative logarithm of the reaction rate of vitamin B_6 photooxidation on the negative logarithm of the concentration of copper ions in the system under the influence of UV radiation. [B_6] = *const.* = $3 \cdot 10^{-4}$ M; [H_2O_2] = *const.* = $3 \cdot 10^{-5}$ M. Radiation source: Oriel Solar Simulator, AM1.5D filter [own data]

As a result of the calculations, the partial reaction orders with respect to the concentrations of the system components were determined to be 0.2 for vitamin B_6, 0.4 for hydrogen peroxide, and 0.3 for Cu^{2+} ions. Accordingly, the rate equation describing the photolysis of vitamin B_6 in the studied system can be expressed as follows:

$$W = \kappa \cdot [B_6]^{0.2} \cdot [H_2O_2]^{0.4} \cdot [Cu(II)]^{0.3} \quad (12)$$

The effective rate constant of the process was determined to be k = $(3.91 \pm 0.17) \cdot 10^{-4}$ s^{-1} and is influenced by the temperature and pH of the medium. Based on this value, the half-life of the process was calculated to be 29.2±0.5 min.

Comparison of the kinetic parameters obtained for vitamin B_6 photolysis in the B_6-H_2O_2-Cu^{2+} system with those determined for the B_6-H_2O_2 system, for which the half-life was 31 min, reveals only a slight decrease in the substrate half-life of approximately 2 min (Table 6). This finding indicates that the process is largely governed by the photochemical behavior of pyridoxine, which is present at a concentration of 10^{-4} M, approximately two orders of magnitude higher than that of copper ions. Under these conditions, Cu^{2+} does not appear to exhibit significant catalytic activity.

Table 6. Effective constant and half-life of pyridoxine (vitamin B_6) photolysis under various conditions [own data]

System	Effective constant (k), s^{-1}	Half-life ($\tau_{½}$), min
Pyridoxine-hv	$(5.38\pm0.25)\cdot10^{-4}$	21.0±0.5
Pyridoxine-H_2O_2-hv	$(3.69\pm0.11)\cdot10^{-4}$	31.1±0.3
Pyridoxine-H_2O_2-Cu(II)-hv	$(3.91\pm0.17)\cdot10^{-4}$	29.2±0.5

Analysis of the literature data indicates that several products may be formed during the photodegradation of vitamin B_6 in the presence of hydrogen peroxide and Cu^{2+} ions under neutral conditions (Table 7).

Table 7. Possible products of photolysis of pyridoxine in the presence of H_2O_2 and ions of Cu^{2+}

Product	Main mechanism	Role of H_2O_2 / Cu^{2+} / light	Bibliographic source
Pyridoxal (4'-aldehyde)	Oxidation of the primary hydroxymethyl group (–CH_2OH) to an aldehyde via •OH attack or one-electron oxidation of radical intermediates	•OH produced by Cu(II)/H_2O_2 (Fenton-like system) or photogenerated ROS oxidize the side chain; irradiation can photoreduce Cu(II) to Cu(I), enhancing ROS generation	[4, 11, 26]
Isopyridoxal / isomeric aldehydes	Radical-induced isomerization and intramolecular hydrogen transfer following excitation or radical attack	The radical pool (•OH, O_2•$^-$) generated from H_2O_2/Cu promotes molecular rearrangements; photochemical excitation increases excited-state species	[11, 26]
Pyridoxi-quinone (oxidized pyridine ring, 3,6-quinone derivatives)	Sequential electron/ proton abstractions from ring followed by O_2 addition and dehydrogenation to give quinone-like structures	Strong oxidants (•OH and photogenerated ROS) promote aromatic ring oxidation; Cu/H_2O_2 systems accelerate deeper oxidative transformation	[11, 28, 29]
Hydroxylated derivatives (6-OH-pyridoxine etc.)	•OH addition to the aromatic ring producing mono- and polyhydroxylated product	•OH generated in Fenton-like Cu/H_2O_2 systems are the main oxidizing agents; these processes increase the •OH flux under near-neutral pH when Cu redox cycling occurs	[30-37]
Demethylated / dealkylated fragments	Homolytic cleavage of C–C or C–O bonds in excited states or via radical attack, leading to loss of	Radical-induced bond scission is enhanced by high ROS concentrations; Cu-catalyzed peroxygenation may produce	[27, 31]

Product	**Main mechanism**	**Role of H_2O_2 / Cu^{2+} / light**	**Bibliographic source**
	methyl or hydroxymethyl fragments	selective C–H hydroxylation followed by bond cleavage	
Pyridoxic acid and other carboxylic fragments	Oxidation of aldehyde intermediates to carboxylic acids; further oxidation and ring cleavage produce small organic acids	High oxidative load (sustained •OH flux) promotes deeper oxidation and partial mineralization; photo-assisted Cu redox cycling increases the extent of transformation	[11, 26]
Low-molecular-weight carbonyls, short-chain acids, CO_2	Progressive oxidative fragmentation and ring opening produce small carbonyl compounds and acids, eventually leading to mineralization to CO_2	Enhanced by sustained ROS generation in Cu/H_2O_2 systems and photo-Fenton-like processes; the extent depends on irradiation time and reagent concentrations	[30]

To confirm the formation and identity of these products, future investigations should be carried out using modern methods and analytical techniques.

CONCLUSIONS

Although vitamin B_6 undergoes measurable direct photolysis under simulated solar irradiation, its highly subunitary quantum yield indicates that direct photolysis is likely negligible under natural aquatic conditions. The presence of hydrogen peroxide and Cu(II) ions decreases the photodegradation rate of pyridoxine, possibly due to competition for UV photons and quenching of the excited states of PN, without efficient generation of reactive radicals in neutral solution. This phenomenon requires further investigation to identify the degradation products formed and to elucidate the underlying mechanisms of the process.

These results demonstrate the involvement of vitamin B_6 in the photochemical self-purification processes occurring in the surface layers of aquatic systems. Such participation may contribute to the restoration of the original properties of aquatic environments when vitamin B_6 enters these systems as a pollutant. Nevertheless, further comprehensive studies are required to fully clarify its environmental fate and role in aquatic photochemical processes.

EXPERIMENTAL SECTION

To investigate the behavior of vitamin B_6 (pyridoxine) in water under irradiation, model systems were constructed according to the 'simple-to-complex' principle. The simplest system consisted of a vitamin B_6 aqueous solution representative of that encountered in natural surface waters. The substrate concentration studied was of the order of 10^{-4} M, and the pH was maintained at 7.0. To ensure constant pH values, a buffer solution of pH 7.0 (25°C in H_2O) consisting of disodium hydrogen phosphate/potassium dihydrogen phosphate, produced by Sigma-Aldrich, was used.

These conditions were simulated in the laboratory using a Solar Simulator Oriel Model 9119X equipped with an Air Mass 1.5 Direct (AM1.5D) filter, which reproduces the solar energy flux and the spectral distribution of UV radiation reaching the Earth's surface when the Sun is positioned at approximately 48.2° from the zenith.

To study the kinetics of vitamin B_6 phototransformations in aqueous solution, a direct spectrophotometric method was employed using a phosphate buffer at pH 7. The absorbance of the solution was measured at 328 nm in order to determine the substrate concentration. Under laboratory conditions, the following photochemical systems were modeled: vitamin B_6-$H_2O_{dist.}$-O_2-hv (1); vitamin B_6-$H_2O_{dist.}$-O_2-H_2O_2-hv (2); *vitamin* B_6-$H_2O_{dist.}$-O_2-H_2O_2-*Cu(II)*-hv (3). All systems were investigated under aerobic conditions.

Hydrogen peroxide (H_2O_2), a naturally occurring oxidant in surface waters, was added in system (2). The inclusion of copper(II) compounds in system (3) was justified by their environmental relevance and by the catalytic role of Cu(II) ions in redox transformations of pollutants.

Kinetic relationships were studied for each modeled system by varying the concentration of a single component while keeping the others constant. All experiments were performed in triplicate, and the results are presented as the arithmetic means. In the kinetic studies, the initial reaction rates were determined within the first 300 s (W_{300}). This time interval was selected due to the relatively rapid degradation of the substrate and to highlight the characteristics of the initial stage of the process, which corresponds to the maximum reaction rate. Based on these data, partial reaction orders were determined, rate equations were derived, and effective rate constants together with substrate half-lives were calculated. The effective rate constant is presented in the form (k±Δk), where Δk represents the absolute measurement error, calculated according to the following relationship:

$$\frac{\Delta k}{k} = \frac{\Delta t}{t} + \frac{\Delta A}{A_0 \cdot 2.3 \cdot log\frac{A_0}{A}} + \frac{\Delta A}{A \cdot 2.3 \cdot log\frac{A_0}{A}} \quad (13)$$

where: Δk – the absolute measurement error (s^{-1}); k – the effective rate constant (s^{-1}); Δt – the absolute error in time measurement (s); t – time (s); ΔA – the absolute error in absorbance measurement; A_0 – the absorbance at time 0; and A – the absorbance at time t.

The concentrations of the components in the model systems were chosen to approximate natural conditions, except for vitamin B_6: hydrogen peroxide at approximately 10^{-5} M, Cu(II) ions at approximately 10^{-6} M, and vitamin B_6 at 10^{-4} M, ensuring appropriate optical density values for spectrophotometric measurements. The numerical data obtained from these experiments are presented in Supporting Information Tables S.1–S.6.

Determination of the quantum yield

To determine the light intensity of the radiation sources used in this study, the potassium ferrioxalate(III) chemical actinometer method ($K_3[Fe(C_2O_4)_3]$) was employed [38, 39].

Synthesis of the potassium ferrioxalate(III) chemical actinometer

The preparation of the potassium ferrioxalate(III) chemical actinometer involves the synthesis of the complex $K_3[Fe(C_2O_4)_3]\cdot 3H_2O$. Potassium ferrioxalate crystals were obtained by mixing three volumes of 1.5 M $K_2C_2O_4$ solution with one volume of 1 M $FeCl_3$ solution. The resulting crystals were recrystallized three times at 45°C using warm double-distilled water and subsequently stored in the dark (Eq. 14) [38, 39]:

$$3K_2C_2O_4 + FeCl_3 \rightarrow K_3[Fe(C_2O_4)_3] + 3KCl \quad (14)$$

Green crystals were obtained as a result of the synthesis. For the actinometric measurements, potassium ferrioxalate(III) solutions of 0.006 M, 0.012 M, and 0.015 M were prepared.

Determination of photon flux

The photon flux of the Solar Simulator Oriel 9119X equipped with AM0 and AM1.5D filters was determined using the potassium ferrioxalate(III) chemical actinometer. The actinometer solution consisted of $K_3[Fe(C_2O_4)_3]\cdot 3H_2O$ dissolved in 0.01 N sulfuric acid. Upon irradiation, the following photochemical reactions occur (Eqs. 15 and 16) [38, 39]:

$$Fe(C_2O_4)_3^{3-} \xrightarrow{h\vartheta} Fe^{2+} + C_2O_4^- + 2C_2O_4^{2-} \quad (15)$$

$$Fe(C_2O_4)_3^{3-} + C_2O_4^- \rightarrow Fe^{2+} + 2CO_2 + 3C_2O_4^{2-} \quad (16)$$

A volume V_1 of the actinometer solution was irradiated for a time interval t. Subsequently, a volume V_2 of the irradiated solution (usually 1 mL) was transferred into a 25 mL volumetric flask (V_3). Then, (10 – V_2) mL of 0.1 N sulfuric acid, 2 mL of 0.1% aqueous 1,10-phenanthroline solution, and 5 mL of acetate buffer solution were added.

The volume was adjusted to the mark with double-distilled water, mixed thoroughly, and kept in the dark for 30 min to establish equilibrium. The absorbance of the Fe(II)-1,10-phenanthroline complex was measured at 510 nm. The amount of formed Fe^{2+} ions (υ) was calculated according to Eq. 17 [38, 39]:

$$\nu_{Fe^{2+}} = 10^{-3} \frac{V_1 \cdot V_3 \cdot A}{V_2 \cdot \varepsilon \cdot l} \quad (17)$$

where: V_2 – the volume of irradiated actinometer solution (mL); V_3 – the final dilution volume (mL); A – the absorbance at 510 nm; ε – the molar extinction coefficient at 510 nm ($1.11 \cdot 10^4$ $M^{-1} \cdot cm^{-1}$); l – the optical path length of the cuvette (cm).

The photon flux was calculated according to Eq. 18 [38, 39]:

$$I = 10^{-3} \frac{V_1 \cdot V_3 \cdot A}{V_2 \cdot \varepsilon \cdot l \cdot \Phi \cdot t} \quad (18)$$

where: I – the light intensity (photon flux) emitted by the irradiation source, Einstein$\cdot s^{-1}$; Φ – the quantum yield of potassium ferrioxalate(III).

The irradiation interval (t) was selected to ensure absorbance changes within the range of 0.1 – 0.6 units. For improved accuracy, a blank experiment using a non-irradiated sample was also performed.

Calculation of Quantum Yield and Light Parameters

The light intensity allows the calculation of the quantum yield for photochemical reactions. The quantum yield of product formation (Φ) was determined as the ratio between the amount of product formed (Δv) and the amount of absorbed light (ΔI_a), during the irradiation time (t) [38, 39]:

$$\Phi = \frac{\Delta \nu}{\Delta I_a \cdot t} \quad (19)$$

The average light intensity (photon flux) emitted by the irradiation source ($I_{avg.}$) was calculated according to Eqs. 20 and 21 [38, 39]:

$$I_{avg.} = \frac{\Delta\nu(Fe^{2+})}{\Delta t \cdot \Phi} \quad (20)$$

where: $I_{avg.}$ – the average light intensity emitted by the irradiation source, (Einstein·s^{-1}); $\Delta\nu$ (Fe^{2+}) – the amount of Fe^{2+} formed after irradiation (mol); Δt – the irradiation time (s); and Φ is the quantum yield.

$$I_{avg.} = \frac{\Delta\nu(Fe^{2+})\cdot 1000}{\Delta t \cdot \Phi \cdot V_s} \quad (21)$$

where: V_s – the irradiated sample volume (mL), and 1000 – the conversion factor from mL to L.

The luminous flux (Einstein·cm^{-2} ·min^{-1}) was calculated according to Eq. 22 [38, 39]:

$$Luminous\ flux = \frac{I_{avg.}\cdot 60}{S} \quad (22)$$

where: S – the irradiated surface area (cm^2); and 60 – the conversion factor from seconds to minutes.

The energy flux (J·cm^{-2}·min^{-1}) was determined according to Eq. 23 [38, 39]:

$$Energy\ flux = \frac{Luminous\ flux \cdot j \cdot h \cdot c \cdot 10^9 \cdot 100}{\lambda} \quad (23)$$

where: j – the number of photons per Einstein ($6{,}02\cdot10^{23}$); h – Planck's constant ($6{,}626\cdot10^{-34}$ J·s); c – the speed of light ($3\cdot10^8$ m·s^{-1}); and λ – the wavelength of light (nm).

ACKNOWLEDGMENTS

The results have been obtained in the framework of the projects funding from the Ministry of Education and Research of the Republic of Moldova (project 010603 – Advanced research in computational and ecological chemistry: identification of technological procedures for water treatment and formation of water quality and quantity, and project 25.80013.5107.20ROMD – New redox and coordination chemistry with cobalamin and related systems (REDOXCOB)) and from the Ministry of Education and Research of Romania (joint funding for project REDOXCOB – PN-IV-PCB-RO-MD-2024-0515, contract no. 52PCBROMD/2025).

The authors thank Dr. Cezara Zagrean-Tuza and Nicoleta Andrian (UBB) for helpful discussions.

REFERENCES

1. L. P. Barada; L. Cutter; J. P. Montoya; E. A. Webb; D. G. Capone; S. A. Sañudo-Wilhelmy, *Front. Microbiol.*, 2013, 4, 25, DOI: 10.3389/fmicb.2013.00025.
2. M. A. Sneineh, *Nutr. Res. Food Sci. J.*, 2021, 4(1), 1–9, DOI: 10.31038/NRFSJ.2021411.
3. P. Bilski; M. Y. Li; M. Ehrenshaft; M. E. Daub; C. F. Chignell, Vitamin B6 (Pyridoxine) and Its Derivatives Are Efficient Singlet Oxygen Quenchers and Potential Fungal Antioxidants. *Photochemistry and Photobiology*, 2007, DOI: 10.1562/0031-8655(2000)0710129SIPVBP2.0.CO2.
4. J. Natera; W. Massad; N. A. García, The role of vitamin B6 as an antioxidant in the presence of vitamin B2-photogenerated reactive oxygen species. A kinetic and mechanistic study. *Photochem. Photobiol. Sci.*, 2012, 11(6), 938–945, DOI: 10.1039/c2pp05318g.
5. A. H. Merrill Jr; J. M. Henderson, Vitamin B6 metabolism by human liver. *Ann. N. Y. Acad. Sci.*, 1990, 585, 110–117, DOI: 10.1111/j.1749-6632.1990.tb28047.x.
6. R. Percudani; A. Peracchi, A genomic overview of pyridoxal-phosphate-dependent enzymes. *EMBO Rep.*, 2003, 4(9), 850–854, DOI: 10.1038/sj.embor.embor914.
7. R. G. Wilson; R. E. Davis, Clinical chemistry of vitamin B6. *Adv. Clin. Chem.*, 1983, 23, 1–68, DOI: 10.1016/s0065-2423(08)60397-2.
8. A. C. Eliot; J. F. Kirsch, Pyridoxal phosphate enzymes: mechanistic, structural, and evolutionary considerations. *Annu. Rev. Biochem.*, 2004, 73, 383–415, DOI: 10.1146/annurev.biochem.73.011303.074021.
9. Gh. Duca; Iu. Scurlatov, *Ecological Chemistry*, Publishing Center M.S.U., Chisinau, 2002, 279 pp., ISBN: 9947-70-172-8.
10. M. S. Aleksevnina; I. V. Pozdnev, *Sanitary Hydrobiology with Fundamentals of Aquatic Toxicology: Textbook*, Perm State National Research University, Perm, 2016, 205 pp., ISBN: 978-5-7944-2769-1.
11. H. Reiber, Photochemical reactions of vitamin B6 compounds, isolation and properties of products. *Biochim. Biophys. Acta*, 1972, 279(2), 310–315, DOI: 10.1016/0304-4165(72)90148-1.
12. D. W. Brousmiche, et al., Photogeneration of quinone methide-type intermediates from vitamin B6. *J. Org. Chem.*, 2002, 67(2), 559–566, DOI: 10.1016/S1010-6030(01)00654-2.
13. M. Wu; Q. Xu; A. Strid; J. M. Martell; L. A. Eriksson, Theoretical study of pyridoxine (vitamin B6) photolysis. *J. Phys. Chem. A*, 2011, 115(46), 13556–13563, DOI: 10.1021/jp205724k.
14. P. Bilski; M. Y. Li; M. Ehrenshaft; M. E. Daub; C. F. Chignell, Vitamin B6 (pyridoxine) and its derivatives are efficient singlet oxygen quenchers and potential fungal antioxidants. *Photochem. Photobiol.*, 2000, 71(2), 129–134, DOI: 10.1562/0031-8655(2000)071<0129:SIPVBP>2.0.CO;2.

15. H. Ikai; K. Nakamura; M. Shirato; T. Kanno; A. Iwasawa; K. Sasaki; Y. Niwano; M. Kohno, Photolysis of hydrogen peroxide, an effective disinfection system via hydroxyl radical formation. *Antimicrob. Agents Chemother.*, 2010, 54(12), 5086–5091, DOI: 10.1128/AAC.00751-10.
16. R. Joshi; S. Adhikari; T. Mukherjee, Pulse radiolysis studies on pyridoxine. *Res. Chem. Intermed.*, 2002, 28(8), 703–713, DOI: 10.1163/15685670260373272.
17. R. J. Yang, et al., Vitamin B6 metabolism and biomarkers. *Animals*, 2023, 13(8), 1333, DOI: 10.3390/ani13081333.
18. J. M. Matxain, et al., Reactivity of vitamin B6 towards hydroxyl radicals. *J. Phys. Chem. A*, 2009, 113(28), 8010–8017, DOI: 10.1021/jp903023c.
19. B. K. Ohta; C. S. Foote, Characterization of pyridoxine endoperoxides and peroxides. *J. Am. Chem. Soc.*, 2002, 124(46), 12064–12065, DOI: 10.1021/ja0205481.
20. W. H. Glaze; J. W. Kang; D. H. Chapin, The chemistry of water treatment processes involving ozone, hydrogen peroxide and UV-radiation. *Ind. Eng. Chem. Res.*, 1995, 34(7), 2314–2323, DOI: 10.1021/ie00046a013.
21. S. L. Murov; I. Carmichael; G. L. Hug, *Handbook of Photochemistry*, 2nd ed.; CRC Press, 1993.
22. G. V. Buxton; C. L. Greenstock; W. P. Helman; A. B. Ross, *J. Phys. Chem. Ref. Data*, 1988, 17(2), 513–886.
23. J. J. Pignatello; E. Oliveros; A. MacKay, Advanced oxidation processes for organic contaminant destruction. *Crit. Rev. Environ. Sci. Technol.*, 2006, 36(1), 1–84.
24. I. Mansilla-Rivera; J. O. Nriagu, Copper Chemistry in Freshwater Ecosystems: An Overview. *J. Great Lakes Res.*, 1999, 25(4), 599–610, DOI: 10.1016/S0380-1330(99)70765-3.
25. G. Albarrán; F. Ramírez-Cahero; R. Aliev, Radiolysis of pyridoxine (vitamin B6) in aqueous solution under different conditions. *Radiat. Phys. Chem.*, 2008, DOI: 10.1016/j.radphyschem.2007.09.013.
26. P. N. Moorthy; E. Hayon, One-electron redox reactions of water-soluble vitamins. III. Pyridoxine and pyridoxal phosphate (vitamin B6). *J. Am. Chem. Soc.*, 1975, DOI: 10.1021/ja00841a009.
27. R. Joshi; S. Kapoor; T. Mukherjee, Free radical reactions of pyridoxal (vitamin B6): A pulse radiolysis study. *Res. Chem. Intermed.*, 2002, DOI: 10.1163/15685670260373272.
28. K. Aoki, et al., Crystal structure of a photolysis product of vitamin B6: A pyridodihydrofuran-condensed skeleton compound of pyridoxal 5'-phosphate. *J. Mol. Struct.*, 2017, DOI: 10.1016/j.molstruc.2017.06.068.
29. M. Pérez-Moya; T. Kaisto; M. Navarro; L. J. del Valle, Study of the degradation performance (TOC, BOD, and toxicity) of bisphenol A by the photo-Fenton process. *Environ. Sci. Pollut. Res.*, 2016, DOI: 10.1007/s11356-016-7386-6.
30. I. Garcia-Bosch, et al., Copper-catalyzed oxidation of alkanes with H2O2 under mild conditions. *Angew. Chem. Int. Ed.*, 2016, DOI: 10.1002/anie.201607216.
31. J. W. Moffett; R. G. Zika, Reaction kinetics of hydrogen peroxide with copper and iron in seawater. *Environ. Sci. Technol.*, 1987, DOI: 10.1021/es00162a012.

32. B. Kim, et al., Fenton-like Chemistry by a Copper(I) Complex and H2O2 Relevant to Enzyme Peroxygenase C–H Hydroxylation. *J. Am. Chem. Soc.*, 2023, DOI: 10.1021/jacs.3c02273.
33. L. Wang, et al., A review on advanced oxidation processes: mechanisms, catalysts and optimizations. *Chem. Eng. J.*, 2022, DOI: 10.1016/j.cej.2021.132108.
34. S. Hussain, et al., A review of copper-based Fenton reactions for the removal of organic pollutants from wastewater over the last decade. *Environ. Sci. Pollut. Res.*, 2021, DOI: 10.1007/s11356-021-16097-0.
35. D. Kahoun, et al., Development and validation of an LC-MS/MS method for quantification of vitamin B6 vitamers in seafood. *J. Food Compos. Anal.*, 2022, DOI: 10.1016/j.jfca.2022.104518.
36. R. J. Yang, et al., Phosphate, 4-pyridoxine acid and pyridoxal in animal tissues: LC/MS identification. *J. Chromatogr. B*, 2023, DOI: 10.1016/j.jchromb.2015.07.008.
37. S. A. Walling, Fenton and Fenton-like wet oxidation for degradation of organic wastes: a critical review. *npj Mater. Degrad.*, 2021, DOI: 10.1038/s41529-021-00192-3.
38. A. Lis. Direct photolysis of cysteine and thiourea in aqueous solutions. Studia Universitatis Moldaviae, 2016, 6(96), 133–141. ISSN 1814-3237.
39. A. Lis; V. Gladchi; S. Travin. Direct photolysis of some thiol substances in the aquatic environment and their role in ecochemical processes in natural waters. Chisinau: CEP USM, 2022, pp. 200–219. ISBN 978-9975-159-05-0.